MARK J. MAYR and JEFFERY W. WARREN

A VISIBLE LASER POSITION SENSOR FOR TESTING A PRECISION LASER BEAM DIRECTOR

A Visible Laser Position Sensor and related equipment were developed to score independently the pointing and tracking performance of a precision laser beam director, and to assess the effect of potential beam-director improvements. The equipment was successfully used to characterize the performance of the Sea Lite Beam Director when transmitting with a low power laser. Tests were conducted at fixed ground sites and on board a helicopter.

INTRODUCTION

During the past 20 years, the Navy has been developing and field testing experimental high-energy laser weapons systems. APL supports the Navy's Strategic Defense Systems Program Office in that effort, in the area of precision tracking and pointing. The Sea Lite Beam Director (SLBD), developed by Hughes Aircraft Company, is an experimental system that directs a high-energy chemical laser at air threats in support of the Navy's short-range air defense mission. The SLBD was installed at the High Energy Laser System Test Facility, a land-based test site at White Sands Missile Range in New Mexico, for performance testing. Subsequently, the program was funded by the Strategic Defense Initiative Organization to perform research on precision pointing and high-energy beam propagation in support of the Strategic Defense Initiative mission. The system was renamed the Sky Lite Beam Director; the new mission is hereafter referred to as the Sky Lite mission.

Much of the initial testing of pointing and tracking performance is done using a low-power visible diagnostic laser instead of the high-energy chemical laser, resulting in eased test logistics and reduced cost. The Visible Laser Position Sensor (VLPS) independently measures beam-on-target error when the low-power diagnostic laser is used. The VLPS is also used to explore design improvements and research the ability of the SLBD to track in the presence of beam wander angle disturbances caused by turbulence, in support of the Sky Lite mission.

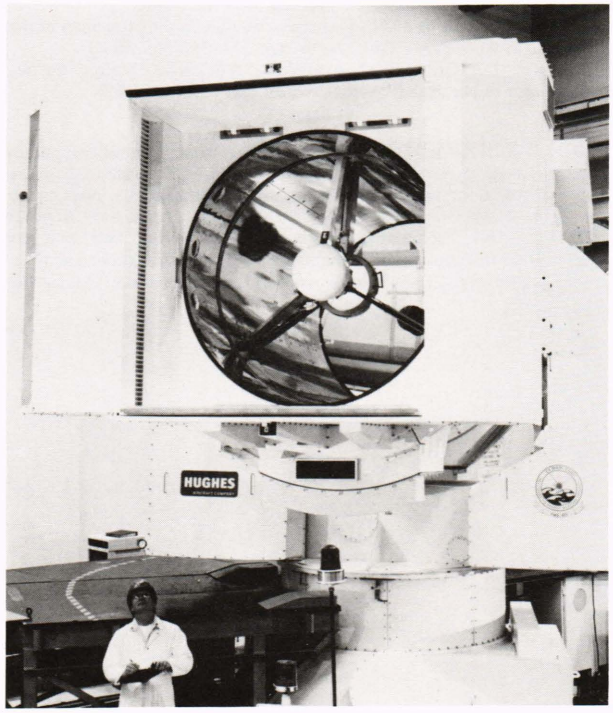

Figure 1—Navy/Hughes Aircraft Sea Lite Beam Director.

SLBD DESCRIPTION

The SLBD (Fig. 1) is a fairly large beam director that uses a 1.8-m-diameter primary mirror in the beam expander. Fine pointing and tracking accuracies are achieved by linking the off-axis tracker line of sight and the high-power beam line of sight to an inertially stabilized platform via a sophisticated alignment system that uses low-power alignment laser beams and several beam-steering mirrors. The inertially stabilized platform (beneath the white cover at the center of the beam expander in Fig. 1) also contains an Independent Inertial Reference Unit (IIRU). The IIRU, a test instrument also developed by APL, is used to measure the motion of the stabilized platform, which is a good approximation of the motion of the high-power beam in inertial space if the errors in the SLBD alignment system described above are small.

The SLBD uses either a forward-looking infrared (FLIR) tracker or a visible television (TV) tracker to provide pointing-error information. The tracker algorithms allow pointing of the beam either at the track point or at an aim point that is offset from the track point. Various tracking modes, such as centroid track or correlation track, are available.

Laser pointing errors result from several sources. Noise in the tracker (either FLIR or TV) and processing electronics or in the alignment systems will cause errors

in the position of the laser spot. Atmospheric turbulence causes errors both in tracking (by causing changes in the apparent position of the target) and in pointing (by causing the transmitted laser beam to wander). If the bandwidth of the pointer/tracker is sufficiently high and the line of sight of the tracking and beam-pointing systems is coincident (a shared optical aperture for both systems), then the turbulence-induced error introduced in the tracker path is compensated for by the error introduced in the pointer path. This technique is planned for use in the Sky Lite configuration. In addition to causing the beam to wander, turbulence also causes beam spread, which reduces the irradiance in the spot by spreading the spot over a larger area. Another error source is static misalignment of the pointer and tracker line of sight. Such misalignment can be a function of the look angle of the SLBD. Target and track-loop dynamics can also introduce errors in some cases.

Errors in pointing the SLBD are classified according to their frequency components. Boresight is a static error. Although boresight errors can be large, they can be compensated for with a one-time correction. Dynamic errors with frequencies less than 1 Hz are referred to as trend. Trend can be caused by tracking a moving target if the pointer/tracker boresight error is a function of look angle. Errors above 1 Hz are referred to as jitter. In missions conducted to date, jitter reduction has been a key technical challenge. Although the VLPS is used to measure boresight, trend, and jitter, the primary objective is to measure jitter very accurately.

VLPS TESTING

The tests that use the VLPS can be grouped into three categories: static tests, dynamic tests, and the high-bandwidth tracking experiment. Each of the three tests imposes different system requirements on the design of the VLPS and related equipment. With minor component and configuration variations, the VLPS instrumentation is designed to satisfy the requirements for all the tests. Two versions of the VLPS were constructed: a ground-based VLPS (GVLPS) to meet the requirements of the static tests and the high-bandwidth tracking experiment test, and an airborne VLPS (AVLPS) to meet the requirements of the dynamic tests.

The static tests (Fig. 2a) require that the SLBD acquire and track the GVLPS, and then point the low-power krypton laser at the active scoring area of the VLPS. The range between the SLBD and the GVLPS can vary from 0.5 to 8 km, but the GVLPS is stationary for any given test run. Because pointing and tracking performance of a precision beam director is naturally specified in units of angle and the VLPS measures beam-on-target position error, the position noise for the VLPS equipment is required to be much less than the product of the range and the expected pointing and tracking angle errors, at all ranges of interest. Operation at the

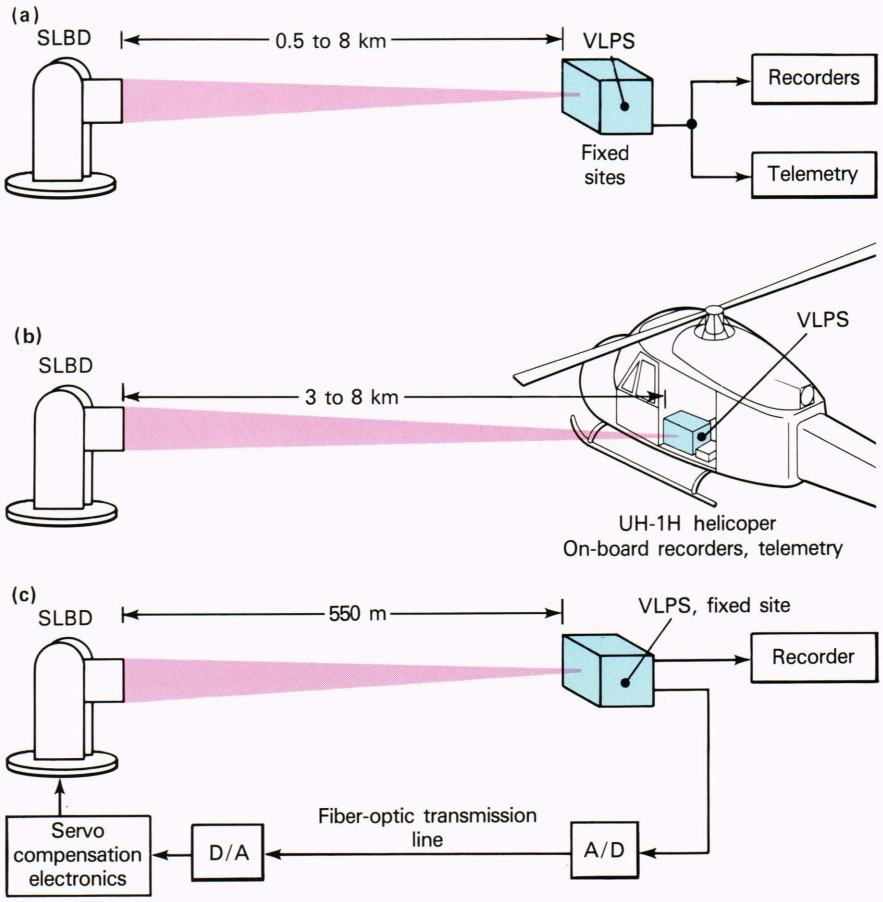

Figure 2—SLBD tests: (a) static tests, (b) dynamic tests, and (c) high-bandwidth tracking experiment.

shortest range requires the lowest position noise for the VLPS, both because a given position noise represents a larger angle at shorter range, and because the best beam-director pointing performance would be expected at the shortest range. Since divergence of the transmitted laser beam and atmospheric turbulence increase the size of the laser spot as the range increases, the active area of the target plane must be large for long-range tests. The tolerable acceptance angle between the laser line of sight and the normal to the GVLPS target plane can be made as small as a few degrees by manually aligning the stationary VLPS to face the SLBD.

The dynamic tests (Fig. 2b) differ from the static tests in several ways. The AVLPS is installed on board a UH-1H helicopter so that crossing target tests can be performed. The ranges of interest lie between 3 and 8 km. The allowable position noise of the AVLPS equipment can be much larger than that required for the static tests because the minimum range is greater. The acceptance angle for the dynamic tests must be as large as 45° to accommodate both the crossing-target engagement geometry and helicopter yaw disturbances caused by crosswinds and pilot corrections.

The high-bandwidth tracking experiment (Fig. 2c) differs substantially from both the static and dynamic tests. The GVLPS is initially acquired and tracked by the SLBD as in the static test, and then a high-bandwidth track loop is closed through the GVLPS via a fiber-optic transmission line to the SLBD servo-compensation electronics. In this experiment, the GVLPS is used as a low-noise, high-bandwidth track-error sensor to explore the performance limits of the beam director for various design improvements, as well as to observe how well the beam director is able to track through beam-wander disturbances caused by turbulence, which is important to the Sky Lite mission. The range is fixed at 550 m. Both the smaller angle-error budget of the SLBD for the Sky Lite mission and the short range levy a consequently smaller position-noise requirement on the GVLPS equipment. Because the GVLPS is part of a closed track loop, the frequency response of the GVLPS is constrained by the allowable phase lag of an ideal Sky Lite tracker.

DESIGN

The VLPS concept (Fig. 3) consists of several major elements. A diffuser screen is the area where the SLBD directs the low-power krypton laser beam. This diffuser scatters incident laser light back to the VLPS sensors such that the received laser power is relatively insensitive to the angle of incidence of the laser beam on the diffuser surface. Large acceptance angles are achieved at the expense of loss of received power. That trade-off is effected by proper selection of the diffuser material for the acceptance angle required by a specific test.

The position sensor assembly consists of an optical interference filter, an imaging lens, a two-axis position detector, and preamplifier electronics. The interference filter passes the krypton laser wavelength of 647.1 nm while suppressing the ambient light from the sun and sky. The preamplified signals are converted into position and

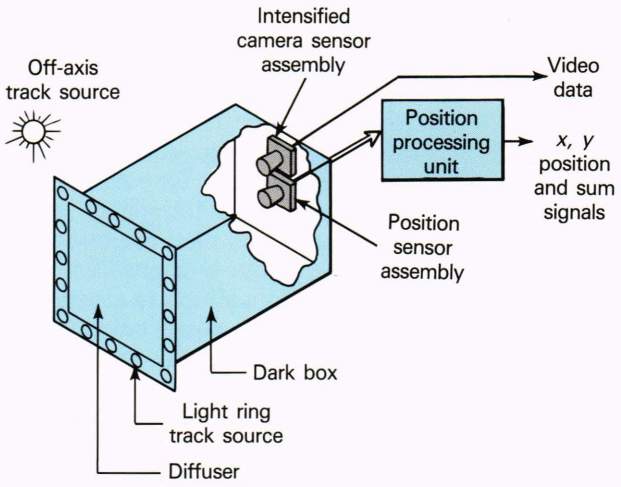

Figure 3—VLPS concept.

sum (received power) signals via the position processing unit. An intensified camera, also filtered by an interference filter, is provided to record beam profile and position, although it is limited to a 30-Hz frame rate. The camera is gated at approximately 500 μs per frame to preclude image blurring.

Two sources are provided as both visible and IR emitters for the SLBD trackers. An off-axis source, consisting of two 250-W tungsten–halogen lamps, allows testing of the ability to point the laser at an aim point (center of the diffuser) that is not colocated with the track point (the lamps). The light ring source, constructed of 28 lights rated at 20 W each arranged in a square ring, allows the SLBD to track the center of the ring using a centroid-track mode and to point the laser at the same point. The light ring also appears as an extended source, which is preferred while operating in certain track modes.

The important VLPS system design constraints that determine the optical and electronic designs are summarized in Table 1.

The krypton ion (Kr^+) laser has a nominal power rating of 0.5 W. Only a small fraction of that power is transmitted from the SLBD because the optics are optimized for the mid-infrared region. A maximum transmitted power of 20 mW was assumed, although typically the laser power transmitted from the SLBD was reduced to 3.5 mW to preserve the laser tube and to ensure eye safety during night flights. The laser is modulated at either 4 or 10 kHz.

OPTICAL SYSTEM

Figure 4 is a diagram of the optical configuration of the VLPS. The lens focuses an image of the diffuser on the detector. For the image to be in focus, the following condition must be met:

$$\frac{1}{F} = \frac{1}{S'} + \frac{1}{S}, \qquad (1)$$

Table 1—VLPS system design constraints.

Test Scenario	*Static*	*Dynamic*	*High-Bandwidth Tracking Experiment*
Operating range (km)	0.5 to 8	3 to 8	0.55
Allowable position noise (mm rms)	0.5	3.0	0.06
Acceptance angle (deg)	±5	±45	±5
Frequency response	≈ 200 Hz (−3 dB)	≈ 200 Hz (−3 dB)	14.57° lag at 40 Hz, second-order Butterworth low-pass at 225 Hz

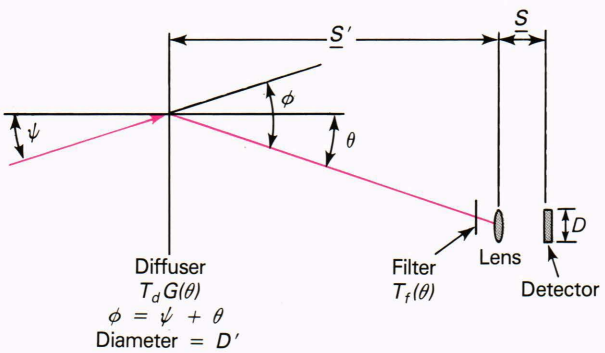

Figure 4—Geometry of VLPS for optical calculations.

where F is the focal length of the lens, S' is the distance from the diffuser to the lens, and S is the spacing from the lens to the detector. All primed dimensions in Fig. 4 are on the diffuser side of the lens, while unprimed dimensions are on the detector side. The magnification M of the image is determined by

$$M = \frac{S}{S'} \quad . \tag{2}$$

The laser beam is incident on the diffuser at angle ψ, which is determined by how well the VLPS is pointed at the SLBD. The diffuser scatters the light so that it may be viewed over a range of angles. The angle θ defines the angle of incidence of the light from the spot onto the lens. (Note that since both the spot and lens have finite dimensions, the angle θ is actually an average for all the light reaching the detector from the spot being considered.) The algebraic sum of θ and ψ gives the angle ϕ through which incident light must be scattered by the diffuser to reach the lens and detector. The diameter of the active area of the detector is given by D. The active area of the diffuser D' is given by

$$D' = \frac{D}{M} \quad , \tag{3}$$

even though the physical dimension of the diffuser is larger. (Regions outside the active area of the diffuser are imaged outside the active area of the detector.)

Diffusers are described by their transmission and gain. The transmission T_d is the fraction of incident light that exits the diffuser on the other side. All light within the exiting hemisphere (solid angle equal to 2π) is collected to measure the transmission. The gain, which is a function of angle, is the light intensity in a given direction divided by the intensity that would occur if the light were scattered uniformly into the hemisphere. Examples of gain characteristics of diffuser materials are illustrated in Fig. 5. For the Lambertian diffuser (Fig. 5a), the gain is not a function of ϕ and is unity throughout the hemisphere. For the high-gain diffuser (Fig. 5b), the gain is very high for $\phi = 0°$, but very small for large values of ϕ. The desire to maximize power received by the detector by using a high-gain diffuser is limited by the maximum angle that must be accommodated. If a wide range of values of ϕ must be accepted, then the power received will vary with this angle significantly for a high-gain diffuser, which affects the required dynamic range of the electronics.

Because of the divergent requirements for ground and airborne testing, we decided to build equipment with different optical configurations for the two sets of tests. Common electronic processing equipment is used for both units. To permit testing over a wide range of angles for the airborne tests, we equipped the AVLPS with a diffuser that has an approximately Lambertian gain characteristic. The diffuser is 0.8-mm-thick Teflon, with $T_d \approx 0.4$, and approximately uniform gain. For the GVLPS diffuser, we selected Mylar drafting paper with a frosted surface.

Figure 6 is a plot of gain versus angle for both diffusers, based on laboratory tests. It is seen that the Mylar diffuser has a gain of 15 at 0°, compared to approximately 1 for the Teflon diffuser. For an angle of 25°, the Teflon diffuser gives more power on target. The Mylar diffuser clearly increases the amount of power that is collected if the angle ϕ can be kept small. It will be recalled that ϕ is equal to the sum of θ and ψ. As discussed previously, ψ can be minimized by carefully aiming the GVLPS at the SLBD. The maximum value of θ is determined by the diameter of the active area of the diffuser and the spacing from diffuser to lens. The diameter of the diffuser is determined by test requirements, while the length of the equipment limits the spacing that can be accommodated without the unit becoming unwieldy. Typically, values of θ of 10° must be accepted. From Fig. 6 it is seen that the gain of the Mylar diffuser varies by over a factor of 2 between 0° and 10°. Such a sharp variation in gain with angle would introduce significant errors because of the range of angles subtended

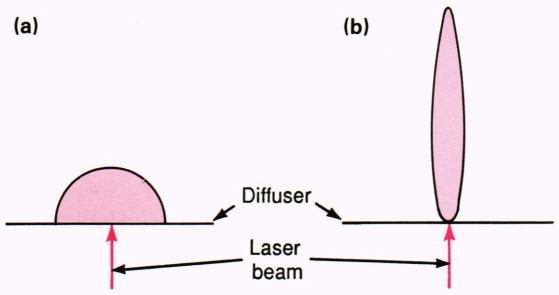

Figure 5—Diffuser gain characteristics: (a) Lambertian and (b) high gain.

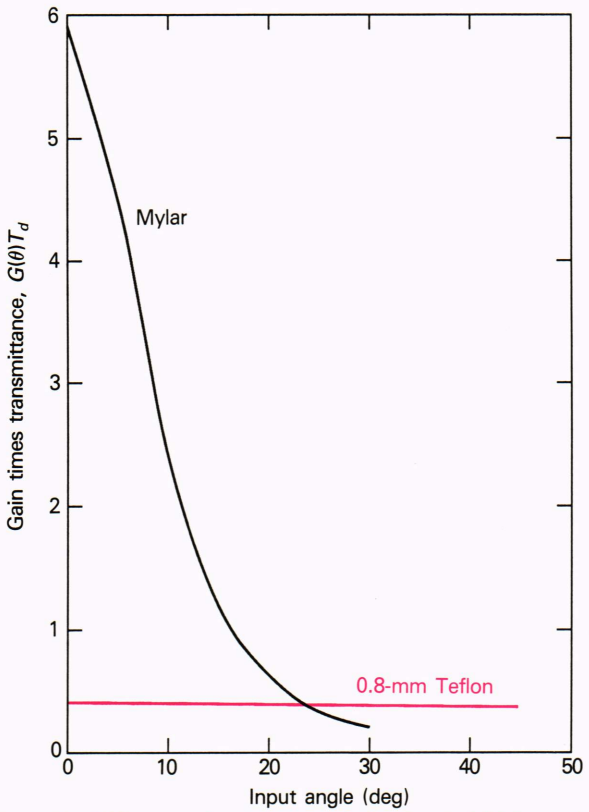

Figure 6—Diffuser gain versus angle for frosted Mylar and 0.8-mm Teflon.

by the spot diameter, as well as increasing the dynamic range requirements.

Fortunately, an optical method is available to effectively negate this angle dependence while retaining the high gain diffuser. If a large-diameter converging lens whose focal length equals the diffuser-to-lens spacing is placed directly behind the diffuser, then the peak gain will be directed toward the receiving lens. A Fresnel lens was used for this purpose in the GVLPS. A Fresnel lens is flat with grooves cut in it such that the angle of the surface at any point has the same slope as that of a conventional lens. The large volume of material in the center of a conventional lens (which does not contribute to the refraction of light rays) is eliminated. While a Fresnel lens has limited quality for imaging applications, it is ideal for energy-direction applications where the incident energy is nearly normal to the lens. A Fresnel lens with a focal length of approximately 1.2 m was incorporated into the GVLPS. The lens is only about 5-mm thick. When the GVLPS was used in the high-bandwidth tracking experiment, the noise requirements were extremely stringent, and the possibility existed of introducing a slight amount of noise because of reflections from the grooves of the Fresnel lens. The Fresnel lens was removed from the high-band-width tracking experiment to eliminate such a possibility. Because the high-bandwidth tracking experiment was a closed-loop test, the laser spot was always centered within a few millimeters, so there was no concern with large θ.

For a given power incident on the diffuser, P_i, we need to calculate the power reaching the detector. The power received by the detector, P_r, can be determined by observing the geometry in Fig. 4. The power from the spot will radiate into the hemisphere behind the diffuser in accordance with the transmission and gain characteristics of the diffuser. The power received is reduced because of the presence of a narrow-band interference filter whose transmission is $T_f(\theta)$, and which was designed to reject sun and sky light. The transmission is a function of angle; the filter is designed with multiple layers that are one-quarter-wavelength thick, with a different index of refraction for each layer. If light enters the filter at an angle, the path length through the layers is no longer exactly a quarter wavelength, and the transmission properties change. If R is the distance from the spot to the lens and A is the area of the lens, then the received power is

$$P_r = P_i \, T_d \, G(\phi) \, T_f(\theta) \, \frac{A \cos\theta}{2\pi R^2} \, . \qquad (4)$$

By using the geometry of the problem and the required conditions for the system to focus the spot on the detector, the power transfer function of the VLPS can be written in terms convenient to the designer as

$$\frac{P_r}{P_i} = \frac{T_d \, G(\phi) \, T_f(\theta) \cos^3\theta}{8 f^2 \, (1 + D/D')^2} \left(\frac{D}{D'}\right)^2 , \qquad (5)$$

where f is the focal length of the lens divided by its diameter. To maximize power, a large detector and small diffuser are needed, although these are constrained by availability and test requirements, respectively. A fast lens (low f) also increases the power received, as would be expected.

Maximum power is desired to minimize the position noise. The equivalent position noise measured at the detector, N_p, can be found by

$$N_p = \frac{I_n \, B^{1/2}}{S_p \, P_r} \, , \qquad (6)$$

where I_n is the noise current density of the detector electronics (in amperes/hertz$^{1/2}$), B is the effective noise bandwidth (in hertz), and S_p is the position sensitivity of the detector (in amperes/watt·centimeter). The quantity of actual interest is the position noise on the diffuser, N_p', which is found from N_p by dividing by the optical magnification, which is equal to D/D'. Thus,

$$N_p' = \frac{I_n B^{1/2} D'}{S_p P_r D} . \quad (7)$$

Equation 7 may be combined with Eq. 4 to yield

$$N_p' = \frac{I_n B^{1/2} 8 f^2 (1 + D/D')^2}{S_p P_i T_d G(\phi) T_f(\theta) \cos^3 \theta} \left(\frac{D'}{D}\right)^3 . \quad (8)$$

System performance trade-offs can be made on the basis of Eq. 8. The inverse-cube dependence of noise on detector diameter leads to the desire to use the largest possible detector. The cubic dependence of noise on diffuser diameter led us to use a smaller diffuser for the GVLPS, where the noise characteristics are the most critical. Once a detector is selected and the diffuser diameter known, the required focal length and the lens-to-diffuser spacing can be determined. The lens was selected from commercial lenses in the desired focal-length range that have low f, and that could be obtained quickly (in order to meet our development schedule), while the spacing was selected to be a convenient length without θ becoming too large. Table 2 shows the selected parameters of the VLPS and the dimensions of each unit.

Table 2—VLPS selected parameters.

Parameter	*GVLPS*	*AVLPS*
T_d	0.85	0.4
$G(\phi = 0)$	15	1
$T_f(\theta)$	0.6	0.75
θ_{max} (deg)	9	9
Focal length (mm)	85	85
f	1.4	1.4
D (cm)	2.5	2.5
D' (cm)	35	45
$(P_r/P_i)\ \|_{\theta=0°}$	2×10^{-3}	5×10^{-5}
P_i (max) (mW)	20	20
P_i (nom) (mW)	3.5	3.5

Electronics

The heart of the VLPS is the two-axis position sensor and subsequent electronic circuits (Fig. 7). The two-axis position sensor is a silicon lateral photo-potentiometer detector. The detector is a five-pin device: the detector bias pin is in the center and the four output pins that define the x and y axes are at the edge of the active area. Current is induced in each pin in proportion to the power of the received laser spot and to the proximity of the spot to that pin. Spot position is estimated by normalizing the difference of two currents from opposing pins by the sum of the same two currents. Although the diameter of the active area of the detector is 4.45 cm, only the central 2.5 cm is used; performance outside that region is too nonlinear to be usable.

The summing and differencing operations for the detector are performed at a carrier frequency of 4 or 10 kHz, depending on whether a chopping wheel or the more accurate Pockels-cell is used to modulate the laser. Processing at a carrier frequency is done because (1) it provides additional rejection of ambient light, (2) there is lower amplifier noise at the carrier frequency, which is important for the trans-impedance amplifiers, and (3) there is rejection of low-frequency disturbances, such as amplifier drift.

The trans-impedance amplifier pair and differencing amplifier for each axis employ matched pairs of precision resistors to minimize drift of the difference signal as functions of temperature and aging. The difference and sum signals, both at the carrier frequency, are amplified prior to transmission over a 3-m cable to the remote position-processing unit.

In the position processor, the sum signal is synchronously demodulated and filtered to provide a DC signal for normalization of the difference signal, and to provide a sum signal output indicative of received power. The difference signal is divided by the DC sum signal to remove the effects of received power fluctuations. The normalized difference signal is then synchronously demodulated and filtered to provide the position measurement.

A reference carrier signal is required for each of the synchronous demodulators in the difference and sum channels for each axis. The reference-generator circuit converts the sum signals from the preamplifier circuit into demodulator reference signals. The signal-to-noise ratio of the sum signals is high enough that the phase noise of the derived reference signals is negligible. The biggest benefit of such a reference-generation technique is that no uplink from the laser modulator to the VLPS is necessary, which is of particular benefit to the helicopter-borne VLPS application.

The three major electronic design areas driven by the system requirements are noise-equivalent position, signal dynamic range, and frequency response.

The noise-equivalent position expression in Eq. 7 contains several terms that are characteristic of the position detector and processing electronics. The bandwidth of the position processing circuit (discussed later) is 225 Hz. The position sensitivity characteristic of the detector is 0.07 A/W·cm.

The total current noise density per detector channel I_N can be computed from

$$I_N = \sqrt{2 (I_{DJ}^2 + I_{DS}^2 + I_{AJ}^2 + I_{AI}^2 + I_{AV}^2)} , \quad (9)$$

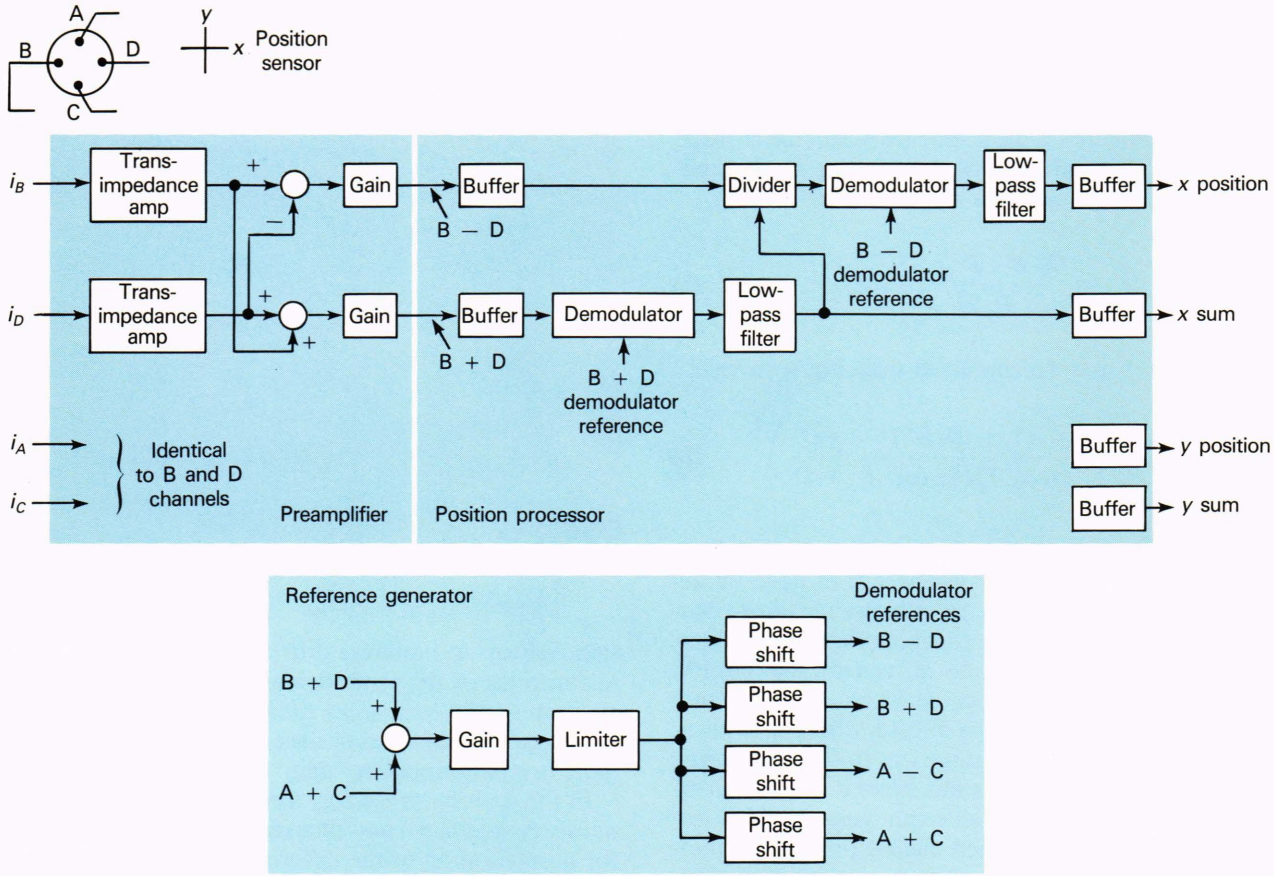

Figure 7—Position electronics functional block diagram.

where

I_{DJ} = Johnson noise of the detector,
I_{DS} = Shot noise of the detector caused by dark current, ambient light, and the received laser power,
I_{AJ} = Johnson noise of the trans-impedance amplifier feedback resistor,
I_{AI} = Current noise of the trans-impedance amplifier,
I_{AV} = Current noise caused by the voltage noise of the trans-impedance amplifier.

The $\sqrt{2}$ term arises because position is derived from the difference of two current signals. The dominant noise sources are I_{DJ} and I_{AV}, although the other terms are not negligible. For the selected detector and low-noise trans-impedance amplifier, $I_N = 4.8 \times 10^{-12}$ A/$\sqrt{\text{Hz}}$. The sensitivity of I_N to received detector power level for the ground and airborne units is negligible.

For the optical design and geometry of the ground-based VLPS unit and nominal laser power, the theoretical N_p' is 0.02 mm rms, which easily meets the requirement for the static and high-bandwidth tracking experiment tests. The theoretical N_p' for the airborne VLPS is 1.1 mm rms, which meets the requirements for the dynamic test. The significant difference in received power for the two units is easily accommodated by gain changes in the preamplifier circuit.

The dynamic range of the position processing circuit, which affects the selection of analog divider, must accommodate the 20:1 variation in the amplitude of the sum signal. The sum signal is a function of received power on the detector and location of the imaged laser spot on the detector. Variation in incident power at the diffuser caused by atmospheric transmittance for the different ranges of interest is estimated conservatively as less than a factor of 2 for the desert environment where the equipment is deployed. By optical design, received power varies by less than a factor of 2 because of the vignetting effects of the interference filter and lens. Finally, the sum signal as a function of spot position on the detector can range from 0.4 to 2 times the amplitude for a centered laser spot, a variation of a factor of 5. A front panel lamp indicates the presence of sufficient sum-signal amplitude for proper circuit operation, an especially helpful aid to the mission operator aboard the helicopter in the busy dynamic test.

The frequency response requirement for the VLPS electronic design is determined both by the track-loop phase-lag requirement for the high-bandwidth tracking experiment and by the desired bandwidth for the static and dynamic tests. The portion of the high-bandwidth tracking experiment track-loop phase lag allocated to the VLPS is 14.6° at 40 Hz. A second-order Butterworth low-pass frequency response with a corner frequency of

225 Hz satisfies the phase lag requirement while allowing an instrumentation bandwidth greater than 100 Hz for the static and dynamic tests.

The frequency response is controlled primarily by the design of the low-pass filter in the position channel (Fig. 7). The selected Butterworth low-pass frequency response also attenuates carrier frequency noise and higher harmonics that result from the synchronous demodulator and other electronic design elements.

AIRCRAFT INTEGRATION

The AVLPS equipment was designed to be flown in a UH-1H helicopter. The aircraft and pilots were supplied by the Army Air Operations Directorate (AAOD) at Holloman AFB, N. Mex. The design of the AVLPS was carefully coordinated with the maintenance division of AAOD to ensure that the installation was compatible with safety requirements and operational procedures. After a trial installation, documentation on the system was submitted to the U.S. Army Aviation Systems Command (AVSCOM) for approval. An airworthiness release was issued by AVSCOM in December 1986, which permitted flight testing to begin.

Figure 8 shows the AVLPS installed in an aircraft. The equipment is compatible with any UH-1H at AAOD. The mission operator is seated facing forward, just behind the pilots, with the control electronics to his left. The mission operator can monitor the data in real time with a TV monitor and oscilloscope and can control all mission systems. His position is also well suited to monitor cockpit instrumentation and to assist the pilot and radar vector controller in assuring that the flight objectives are met.

RESULTS

Laboratory tests were conducted to verify the critical VLPS performance parameters. The equipment was subsequently used in extensive field tests of the SLBD.

Laboratory Tests

Laboratory tests were conducted to measure the position noise, frequency response, and linearity of the GVLPS using a special modulated light source consisting of two sets of light-emitting diodes and modulation electronics. The special modulated light source simulates a laser spot that is either stationary or moving periodically

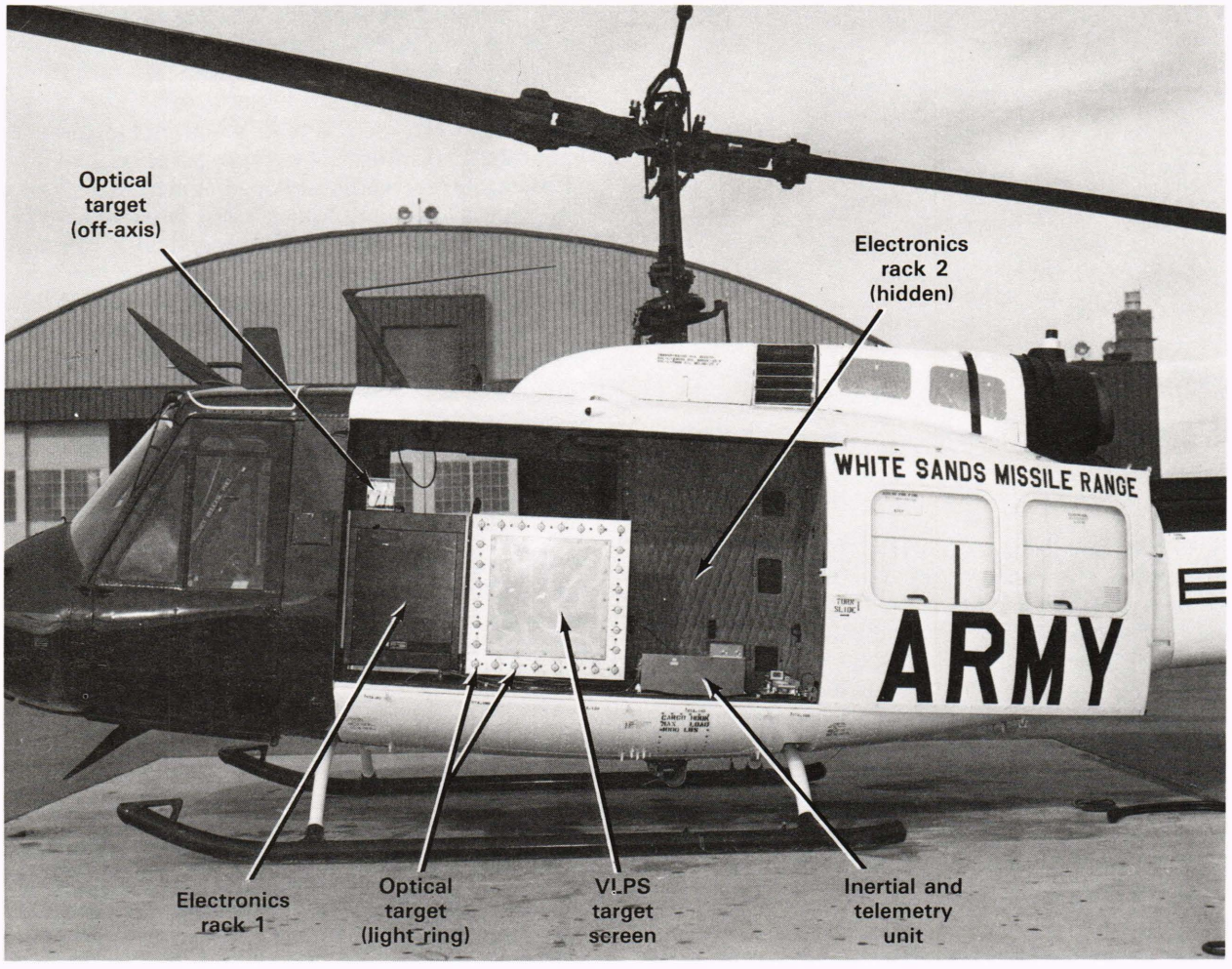

Figure 8—AVLPS mounted in UH-1H helicopter.

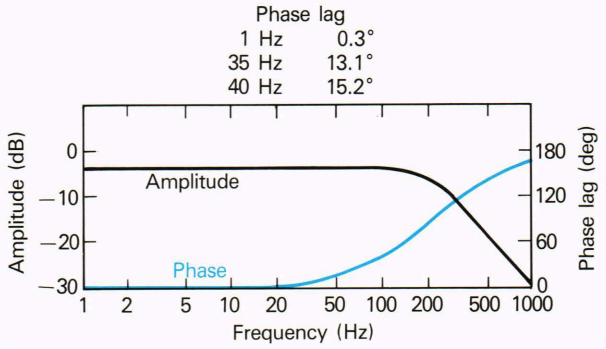

Figure 9—Measured VLPS frequency response for high-bandwidth tracking experiment.

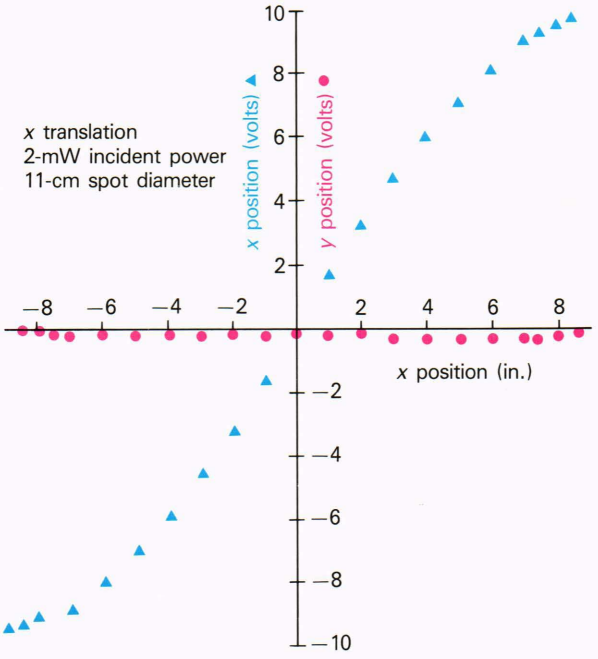

Figure 10—Measured position linearity of VLPS.

across the diffuser. The frequency response of the VLPS matched the design characteristic very well (Fig. 9). The position noise was 0.06 mm rms, which meets the allowable position noise requirement for the high-bandwidth tracking experiment and static tests. The position linearity and cross-axis coupling are shown in Fig. 10.

The position noise for the AVLPS was measured for an earlier generation of the VLPS position processor electronics. The measured position noise of 4 mm rms slightly exceeded the stated requirement for the dynamic test scenario, but was still acceptable given the beam wander caused by atmospheric turbulence, even under benign conditions.

Field Tests

The ground and airborne VLPS systems were used in an extensive series of tests in winter and spring 1987,

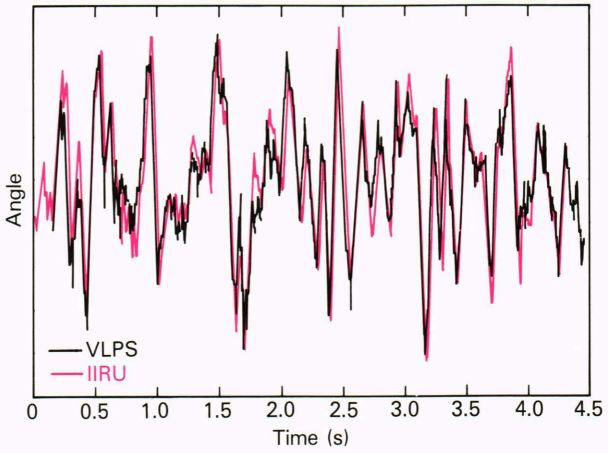

Figure 11—Comparison of jitter measured by AVLPS and IIRU on flight LP4. These data were taken at a range of 3 km and at an aircraft speed of 150 km/h.

in preparation for high power tests in fall 1987. Those were development tests for the SLBD, during which problems with the SLBD were isolated and corrected. Ground testing was used to evaluate basic system performance, especially boresight errors and focus problems. Jitter testing was limited because turbulence is very strong close to the ground, resulting in high levels of jitter induced by turbulence. The ground tests also provided an opportunity to test the data telemetry system, which was supplied to us by the Navy. Airborne tests provided an opportunity to measure the jitter performance of the SLBD against an airborne target. Flight test LP-4, a nighttime flight on 12 March 1987, is particularly interesting because the turbulence conditions measured during the flight were very low. Since turbulence was low, the jitter measured by the AVLPS should have matched that transmitted by the SLBD, as measured by the IIRU. The surprising degree to which these two measurements agree is shown in Fig. 11. During that test the aircraft was flown at an altitude 600 m above the SLBD, with a closest point of approach of 3 km, at a speed of approximately 150 km/h.

Testing for the high-bandwidth tracking equipment was conducted during early 1988. Those tests identified and quantified noise sources in the pointing system of the SLBD when a very-low-noise, high-bandwidth tracker is used. This information will be used in the development of system upgrades to meet the requirements of the Sky Lite mission.

ACKNOWLEDGMENT—We would like to acknowledge the contributions of Ben Hoffman, Roger Lapp, Jim Connelly, and Larry Klein of APL to this effort. Important contributions to this project from people outside APL were made by Virgil Garrett and Bill Bowker of Naval Ordnance Missile Test Station, Jack Rees and Hector Gonzalez of the Army Air Operations Directorate, Earle Neill and George Key of Hughes Aircraft (White Sands), and Randy Thompson of Science Applications International Corporation. We would like to thank Navy engineer Robert Kim for his assistance throughout this project. We would like to especially thank Robert Gray, who worked with us on a daily basis to make this test work, and who operated the equipment himself in our absence.

THE AUTHORS

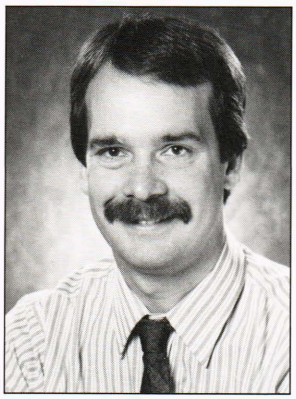

MARK J. MAYR received the B.S.E.E. degree from the Milwaukee School of Engineering in 1978 and the M.S.E.E. degree from The Johns Hopkins University Evening College in 1981. He is a member of APL's Senior Staff and is Section Supervisor of the Electro-Optical Systems Group's Guidance Evaluation Section. Since joining APL in 1978, he has worked on a variety of projects associated with electro-optical, control, and inertial systems. In addition to developing the Sealite Beam Director instrumentation, he managed an improvement effort for a Digital Scene-Matching Area Correlator (DSMAC) signal processor for Tomahawk, analyzed infrared seeker peformance for the rolling airframe missile, developed a two-axis pointer and tracker for the surface-effect ship laser radar instrumentation, and characterized inertial sensors for various projects. He is now working on several electro-optical sensor development tasks for a variety of Laboratory programs. Mr. Mayr is a member of the Society of Photo-Optical Instrumentation Engineers.

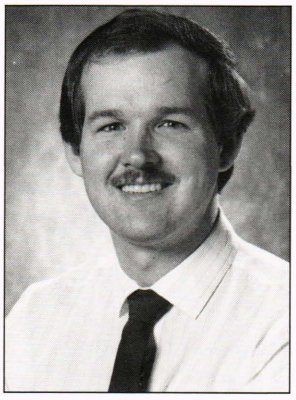

JEFFERY W. WARREN received a B.S. degree in 1981 and an M.S. degree in 1984, both in electrical engineering, from the University of South Carolina. His thesis research evaluated electro-optical measurements of surface charging of insulators in low-frequency electric fields. He joined the Electro-Optical Systems Group in APL's Fleet Systems Department in 1984. Mr. Warren's activities include development and testing of electro-optical systems, and the development of high-power, low-loss, overmoded waveguide.